

# Role of interfering optical fields in the trapping and melting of gold nanorods and related clusters

Hai-Dong Deng,<sup>1,2</sup> Guang-Can Li,<sup>1</sup> Qiao-Feng Dai,<sup>1</sup> Min Ouyang,<sup>1</sup> Sheng Lan,<sup>1,\*</sup>  
Achanta Venu Gopal,<sup>3</sup> Vyacheslav A. Trofimov,<sup>4</sup> and Tatiana M. Lysak<sup>4</sup>

<sup>1</sup>Laboratory of Nanophotonic Functional Materials and Devices, School of Information and Optoelectronic Science and Engineering, South China Normal University, Guangzhou 510006, China

<sup>2</sup>College of Science, South China Agricultural University, Guangzhou 510642, China

<sup>3</sup>Department of Condensed Matter Physics and Material Science, Tata Institute of Fundamental Research, Homi Bhabha Road, Mumbai 400005, India

<sup>4</sup>Department of Computational Mathematics and Cybernetics, M. V. Lomonosov Moscow State University, Moscow 119992, Russia

\*slan@scnu.edu.cn

**Abstract:** We investigate the simultaneous trapping and melting of a large number of gold (Au) nanorods by using a single focused laser beam at 800 nm which is in resonance with the longitudinal surface plasmon resonance of Au nanorods. The trapping and melting processes were monitored by the two-photon luminescence of Au nanorods. A multi-ring-shaped pattern was observed in the steady state of the trapping process. In addition, optical trapping of clusters of Au nanorods in the orbits circling the focus was observed. The morphology of the structure after trapping and melting of Au nanorods was characterized by scanning electron microscope. It was revealed that Au nanorods were selectively melted in the trapping region. While Au nanorods distributed in the dark rings were completely melted, those located in the bright rings remain unmelted. The multi-ring-shaped pattern formed by the interference between the incident light and the scattered light plays an important role in the trapping and melting of Au nanorods.

©2012 Optical Society of America

**OCIS codes:** (350.4855) Optical tweezers or optical manipulation; (350.5340) Photothermal effects; (140.3390) Laser materials processing.

---

## References and links

1. S. Nie and S. R. Emory, "Probing single molecules and single nanoparticles by surface-enhanced Raman scattering," *Science* **275**(5303), 1102–1106 (1997).
2. X. Huang, I. H. El-Sayed, W. Qian, and M. A. El-Sayed, "Cancer cells assemble and align gold nanorods conjugated to antibodies to produce highly enhanced, sharp, and polarized surface Raman spectra: A potential cancer diagnostic marker," *Nano Lett.* **7**(6), 1591–1597 (2007).
3. X. Qian, X. H. Peng, D. O. Ansari, Q. Yin-Goen, G. Z. Chen, D. M. Shin, L. Yang, A. N. Young, M. D. Wang, and S. Nie, "*In vivo* tumor targeting and spectroscopic detection with surface-enhanced Raman nanoparticle tags," *Nat. Biotechnol.* **26**(1), 83–90 (2008).
4. P. Zijlstra, J. W. M. Chon, and M. Gu, "Five-dimensional optical recording mediated by surface plasmons in gold nanorods," *Nature* **459**(7245), 410–413 (2009).
5. J. W. M. Chon, C. Bullen, P. Zijlstra, and M. Gu, "Spectral encoding on gold nanorods doped in a silica sol-gel matrix and its application to high-density optical data storage," *Adv. Funct. Mater.* **17**(6), 875–880 (2007).
6. H. Wang, T. B. Huff, D. A. Zweifel, W. He, P. S. Low, A. Wei, and J. X. Cheng, "*In vitro* and *in vivo* two-photon luminescence imaging of single gold nanorods," *Proc. Natl. Acad. Sci. U.S.A.* **102**(44), 15752–15756 (2005).
7. N. J. Durr, T. Larson, D. K. Smith, B. A. Korgel, K. Sokolov, and A. Ben-Yakar, "Two-photon luminescence imaging of cancer cells using molecularly targeted gold nanorods," *Nano Lett.* **7**(4), 941–945 (2007).
8. X. Huang, I. H. El-Sayed, W. Qian, and M. A. El-Sayed, "Cancer cell imaging and photothermal therapy in the near-infrared region by using gold nanorods," *J. Am. Chem. Soc.* **128**(6), 2115–2120 (2006).

9. I. H. El-Sayed, X. Huang, and M. A. El-Sayed, "Surface plasmon resonance scattering and absorption of anti-EGFR antibody conjugated gold nanoparticles in cancer diagnostics: applications in oral cancer," *Nano Lett.* **5**(5), 829–834 (2005).
10. C. Yu and J. Irudayaraj, "Multiplex biosensor using gold nanorods," *Anal. Chem.* **79**(2), 572–579 (2007).
11. K. M. Mayer, S. Lee, H. Liao, B. C. Rostro, A. Fuentes, P. T. Scully, C. L. Nehl, and J. H. Hafner, "A label-free immunoassay based upon localized surface plasmon resonance of gold nanorods," *ACS Nano* **2**(4), 687–692 (2008).
12. A. Ashkin, "Acceleration and trapping of particles by radiation pressure," *Phys. Rev. Lett.* **24**(4), 156–159 (1970).
13. A. Ashkin, J. M. Dziedzic, and T. Yamane, "Optical trapping and manipulation of single cells using infrared laser beams," *Nature* **330**(6150), 769–771 (1987).
14. A. Ashkin and J. M. Dziedzic, "Optical trapping and manipulation of viruses and bacteria," *Science* **235**(4795), 1517–1520 (1987).
15. C. Selhuber-Unkel, I. Zins, O. Schubert, C. Sönnichsen, and L. B. Oddershede, "Quantitative optical trapping of single gold nanorods," *Nano Lett.* **8**(9), 2998–3003 (2008).
16. M. Pelton, M. Liu, H. Y. Kim, G. Smith, P. Guyot-Sionnest, and N. F. Scherer, "Optical trapping and alignment of single gold nanorods by using plasmon resonances," *Opt. Lett.* **31**(13), 2075–2077 (2006).
17. L. Tong, V. D. Miljković, and M. Käll, "Alignment, rotation, and spinning of single plasmonic nanoparticles and nanowires using polarization dependent optical forces," *Nano Lett.* **10**(1), 268–273 (2010).
18. S. Link, C. Burda, B. Nikoobakht, and M. A. El-Sayed, "How long does it take to melt a gold nanorod," *Chem. Phys. Lett.* **315**(1-2), 12–18 (1999).
19. S. Link, C. Burda, B. Nikoobakht, and M. A. El-Sayed, "Laser-induced shape changes of colloidal gold nanorods using femtosecond and nanosecond laser pulses," *J. Phys. Chem. B* **104**(26), 6152–6163 (2000).
20. S. Link, Z. L. Wang, and M. A. El-Sayed, "How does a gold nanorod melt?" *J. Phys. Chem. B* **104**(33), 7867–7870 (2000).
21. S. Link, C. Burda, M. B. Mohamed, B. Nikoobakht, and M. A. El-Sayed, "Laser photothermal melting and fragmentation of gold nanorods: energy and laser pulse-width dependence," *J. Phys. Chem. A* **103**(9), 1165–1170 (1999).
22. W. Schaertl and C. Roos, "Convection and thermodiffusion of colloidal gold tracers by laser light scattering," *Phys. Rev. E Stat. Phys. Plasmas Fluids Relat. Interdiscip. Topics* **60**(2 2 Pt B), 2020–2028 (1999).
23. R. Spill, W. Köhler, G. Lindenblatt, and W. Schaertl, "Thermal diffusion and Soret feedback of gold-doped polyorganosiloxane nanospheres in toluene," *Phys. Rev. E Stat. Phys. Plasmas Fluids Relat. Interdiscip. Topics* **62**(6 6 Pt B), 8361–8368 (2000).
24. M. M. Burns, J. M. Fournier, and J. A. Golovchenko, "Optical binding," *Phys. Rev. Lett.* **63**(12), 1233–1236 (1989).
25. M. M. Burns, J. M. Fournier, and J. A. Golovchenko, "Optical matter: crystallization and binding in intense optical fields," *Science* **249**(4970), 749–754 (1990).
26. S. A. Tatarikova, A. E. Carruthers, and K. Dholakia, "One-dimensional optically bound arrays of microscopic particles," *Phys. Rev. Lett.* **89**(28), 283901 (2002).
27. A. Haldar, S. B. Pal, B. Roy, A. Banerjee, and S. Dutta Gupta, "Self assembly of microparticles in stable ring structures in an optical trap," *Phys. Rev. A* (to be published).
28. J. Liu, Q. F. Dai, Z. M. Meng, X. G. Huang, L. J. Wu, Q. Guo, W. Hu, S. Lan, A. V. Gopal, and V. A. Trofimov, "All-optical switching using controlled formation of large volume three-dimensional optical matter," *Appl. Phys. Lett.* **92**(23), 233108 (2008).
29. G. Obara, N. Maeda, T. Miyanishi, M. Terakawa, N. N. Nedyalkov, and M. Obara, "Plasmonic and Mie scattering control of far-field interference for regular ripple formation on various material substrates," *Opt. Express* **19**(20), 19093–19103 (2011).
30. G. Obara, Y. Tanaka, T. Miyanishi, and M. Obara, "Uniform plasmonic near-field nanopatterning by backward irradiation of femtosecond laser," *Appl. Phys., A Mater. Sci. Process.* **102**(3), 551–557 (2011).
31. Y. Tanaka, G. Obara, A. Zenidaka, N. N. Nedyalkov, M. Terakawa, and M. Obara, "Near-field interaction of two-dimensional high-permittivity spherical particle arrays on substrate in the Mie resonance scattering domain," *Opt. Express* **18**(26), 27226–27237 (2010).
32. G. Obara, Y. Tanaka, N. N. Nedyalkov, M. Terakawa, and M. Obara, "Direct observation of surface plasmon far field for regular surface ripple formation by femtosecond laser pulse irradiation of gold nanostructures on silicon substrates," *Appl. Phys. Lett.* **99**(6), 061106 (2011).
33. J. W. Yao, C. Y. Zhang, H. Y. Liu, Q. F. Dai, L. J. Wu, S. Lan, A. V. Gopal, V. A. Trofimov, and T. M. Lysak, "High spatial frequency periodic structures induced on metal surface by femtosecond laser pulses," *Opt. Express* **20**(2), 905–911 (2012).

---

## 1. Introduction

With the advance in the nanofabrication and chemical synthesis techniques, metallic particles with various shapes have been synthesized, including nanospheres, nanorods, and nanotriangles etc. In particular, Au nanorods have been widely applied to various fields of science because of the strong absorption and tunability of their longitudinal surface plasmon resonance (LSPR). These applications include surface enhanced Raman scattering [1–3],

multi-dimensional optical storage [4,5], biomedical imaging [6–8], and biosensing etc [9–11]. Accordingly, the manipulation of gold (Au) nanorods and especially the trapping and movement of Au nanorods to the designated places becomes increasingly important. Since the pioneering work of Ashkin by using a single focused laser beam, optical tweezers have been widely used in the trapping of micro- and nanoparticles [12–14]. In the optical trapping of Au nanorods, it has been found that trapped Au nanorods are generally aligned along the polarization of the laser light [15,16]. This unique property has been employed to investigate the rotation of Au nanorods in the optical trap [17]. Due to the strong absorption of laser and the significant enhancement of electric field at the LSPR, Au nanorods can emit strong two-photon luminescence (TPL) when the femtosecond (fs) laser wavelength is in resonance with their LSPR. From another point of view, however, the strong absorption of laser light at the LSPR of Au nanorods leads to the increase of their temperature and even the melting of Au nanorods when the laser fluence exceeds a critical value. In general, the melting of Au nanorods is accompanied with the quenching of TPL [4]. This feature enables us to monitor the trapping and melting processes of Au nanorods. The melting of Au nanorods into nanospheres or smaller nanoparticles has been systematically investigated by El-Sayed *et al* [18–21]. However, the melting of Au nanorods in an optical trap has not been studied.

In this article, we investigated the optical trapping of a large number of Au nanorods by using a single focused laser beam which is in resonance with the LSPR of Au nanorods. The subsequent melting of Au nanorods in an optical trap and the optical trapping of Au clusters in the orbits circling the melted structure were also studied. The TPL image and spectrum of Au nanorods were employed to monitor the trapping and melting processes of Au nanorods. A multi-ring-shaped pattern was observed in the steady state of the trapping process. In addition, optical trapping of clusters of Au nanorods in the orbits circling the focus was observed. The morphology of the structure after trapping and melting of Au nanorods was characterized by scanning electron microscope (SEM). It was revealed that Au nanorods were selectively melted in the trapping region. While Au nanorods distributed in the dark rings were completely melted, those located in the bright rings remain unmelted. It is suggested that the multi-ring-shaped pattern was formed by the interference between the incident light and the scattered light.

## 2. Sample preparation and experimental details

The Au nanorods used in the experiments were purchased from Nanopartz (Salt Lake City, UT). The diameter and length of Au nanorods are 10 and 41 nm, giving a LSPR at ~808 nm. The aqueous solution of Au nanorods with a concentration of 0.0036% (or a molar concentration of 979 pM) was sonicated and injected into a sample cell with a thickness of 50  $\mu\text{m}$ . The sample cell was made of two glass slides. While a conventional cover glass slide was used as the bottom wall of the sample cell, a conductive glass slide was chosen as the upper wall because Au nanorods were going to be trapped and melted at the upper wall of the sample cell and the subsequent morphology characterization by using SEM would become convenient. By doing so, the sputtering of Au, which may affect the morphology of the Au-nanorod-related structure, is not required for SEM observation. The reason why the optical trap for Au nanorods is designed at the upper wall of the sample cell is that the large absorption force acting on Au nanorods in the forward direction has to be balanced by using the upper wall of the sample cell in order to realize steady trapping. The schematic showing the trapping of Au nanorods by fs laser light at the upper wall of the sample cell is shown in Fig. 1. The 800-nm light from a Ti: sapphire laser (Mira 900, Coherent) with a duration of 130 fs and a repetition of 76 MHz was introduced into an inverted microscope (Axio Observer A1, Zeiss) and focused with a 100 $\times$  objective lens (NA = 1.43) on the upper wall of the sample cell or on the lower surface of the conductive glass slide. The TPL emitted from Au nanorods was collected by the same objective lens and analyzed in a spectrometer (SR-500i-B1, Andor) with charge-coupled device (CCD). The trapping and melting processes can be easily monitored by using either the dark-field mode of the microscope or the CCD. Since the laser beam was focused into the aqueous solution of Au nanorods by using an oil-

immersion objective lens, the intensity distribution of the laser beam at the focused spot was examined by using the TPL from the dilute aqueous solution of rhodamine B. A Gaussian distribution of light intensity was observed, implying that both the spherical aberration of the objective lens and the interference between the incident light and the reflected light from the conductive glass can be neglected.

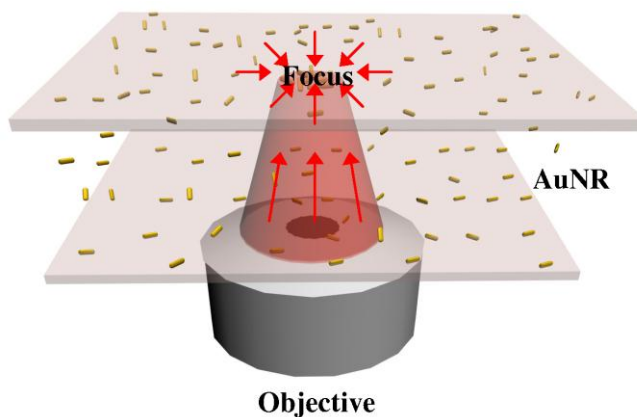


Fig. 1. Schematic showing the trapping of Au nanorods by fs laser light at the upper wall of the sample cell. The arrows indicate the optical forces acting on Au nanorods.

### 3. Results and discussion

#### 3.1 TPL from trapped Au nanorods

TPL emitted by the Au nanorods when the excitation wavelength is set at their LSPR can be used to monitor the Au nanorods entering into the optical trap. The TPL spectra recorded at different times after the switching-on of the laser light are shown in Fig. 2. It can be seen that the TPL intensity of Au nanorods increases rapidly at  $\sim 10$  s after turning on the laser light. After 30 s, the TPL intensity increases nearly one order of magnitude as compared to that at 10 s. It implies that many Au nanorods have been trapped at the focus by the optical forces including gradient forces in the transverse and longitudinal directions and absorption and scattering forces. Of course, the absorption of laser light leads to an increase in the temperature of Au nanorods and the surrounding water, producing a temperature gradient. However, the Soret coefficient of Au nanorods was found to be positive [22,23], implying that Au nanorods will be driven out of the focus due to thermophoresis. Based on experimental observation, the optical forces seem to play a dominant role in determining the movement of Au nanorods and the effects of thermophoresis can be neglected in our experiments.

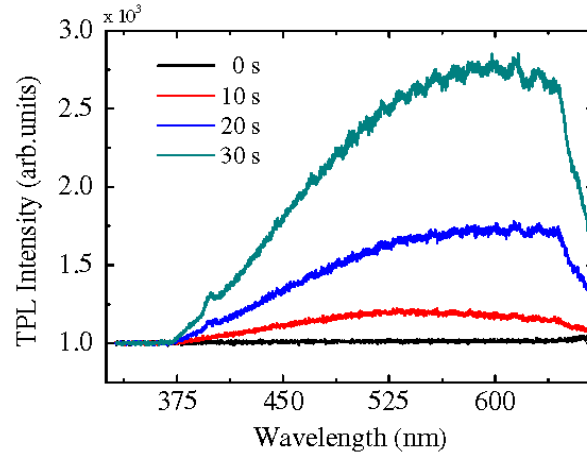


Fig. 2. TPL spectra of trapped Au nanorods recorded at different times after switching on the fs laser.

Relying on the TPL of Au nanorods, the trapping and melting processes of Au nanorods can be monitored by using CCD. The CCD images recorded at different times after switching on the laser light are shown in Fig. 3. Here, it should be emphasized that only Au nanorods oriented in the polarization direction of the laser light can emit strong TPL. At the initial stage, we can see several bright spots moving toward the focus, as shown in Fig. 3(a). The number of bright spots increases rapidly with time and these bright spots tend to form a ring structure, as shown in Figs. 3(b) and 3(c). Finally, a multi-ring-shaped pattern composed of bright and dark rings is observed, as can be seen in Fig. 3(d) where one can find a bright spot surrounded by two bright rings. In most cases, however, the central part of the focus appears to be dark.

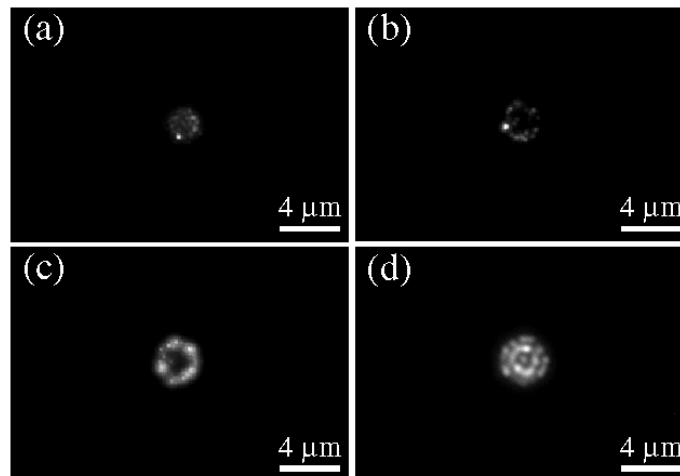


Fig. 3. CCD images without illumination recorded at different times after switching on the laser light, showing the TPL from trapped Au nanorods.

### 3.2 Trapping of Au-nanorod-related clusters in the orbits circling the melted structure

When Au nanorods are trapped at the focus, the high power density of the laser light may lead to the melting of Au nanorods into shorter Au nanorods or Au nanospheres and thus to the significant reduction in TPL because of the blueshift of their LSPR. During this process, the resulting Au nanospheres may coalesce into a big particle at the focus and the subsequent

melting processes will increase the size of this particle. Au nanorods that later enter into the optical trap can only accumulate at the edges of the big particle where the power density is low. Thus, these Au nanorods will remain unmelted and emit strong TPL. This seems the reason why a ring structure with a dark central part is generally observed. At this time, it was found that some clusters of Au nanorods could be steadily trapped in the orbits circling the central particle. In Fig. 4(a), we indicate the central particle and the trapped Au clusters by yellow and red arrows, respectively. It can be seen that the central part of the focus appears to be dark and it is surrounded by a bright ring. In this case, the trapped Au cluster was observed to move randomly in the orbit. We monitored the movement of the trapped Au cluster and noticed that its location was independent of the polarization of the laser light. It was found that Au clusters would be steadily trapped in the orbit once they occasionally entered into the orbit. The steady trapping of two and three Au clusters are shown in Figs. 4(b)-4(d). It seems that there exists a repulsive interaction between the trapped Au clusters, preventing them from coalescing into a large cluster.

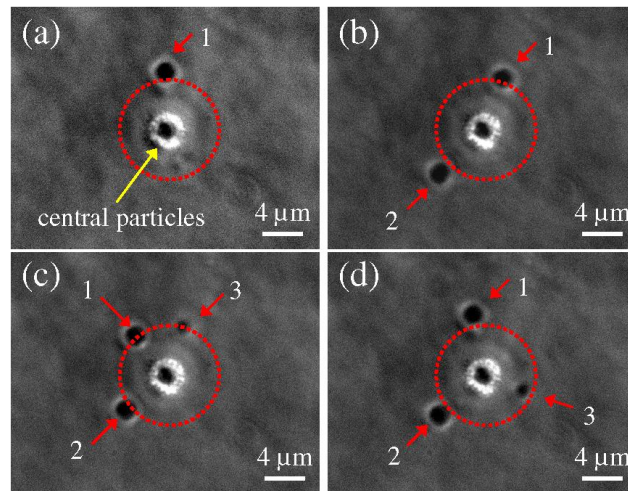


Fig. 4. CCD images with illumination showing one (a), two (b), and three (c and d) Au clusters trapped in the orbit circling the central particle. In each case, the orbit is indicated by a dashed circle.

With increasing time, more and more Au clusters were observed to be trapped in the orbit, as clearly shown in Fig. 5. Apart from the repulsive interaction between the trapped Au clusters that prevents them from coalescing, it was also noticed that there exists an attractive interaction that makes them move as a whole in the orbit. This behavior is clearly shown in Fig. 5 where several Au clusters separated with almost equal distance were observed to move together in the orbit. Similar attraction was observed previously in the optical trapping of dielectric particles and it is referred to as optical binding [24–26]. The physical origin of optical binding is the interference between the trapping light and the scattered light by the particles. A calculation of radial distribution of light field for measurement geometry similar to our setup has shown that the electric field distribution results in formation of rings due to the standing wave pattern that depends on the thickness of the sample cell or the stratified medium [27]. Optical binding plays a crucial role in the formation of optical matters [25,28]. In Figs. 5(c) and 5(d), one can see a cluster with a larger size approaching the orbit. It got trapped in the orbit for some time (see Fig. 5(e)) and eventually became detrapped (see Fig. 5(f)).

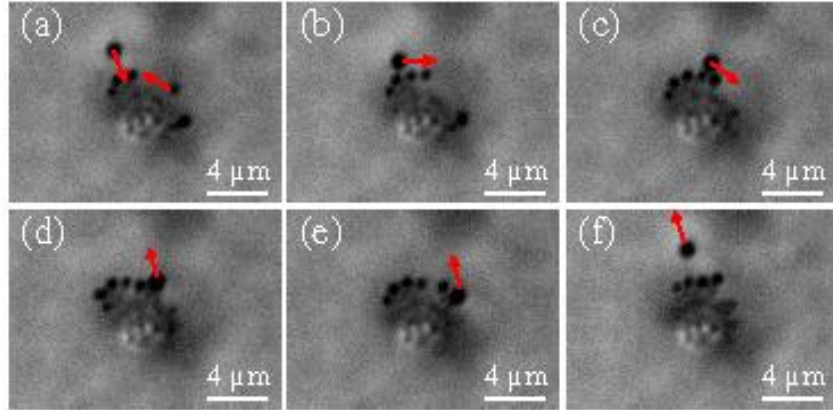


Fig. 5. CCD images with illumination. (a) and (b): two groups of Au clusters that are trapped in the orbit. Each group contains three Au clusters and moves as a whole in the orbit. (c)-(f): A cluster with a larger size (indicated by arrows) approached the orbit ((c) and (d)), got trapped for some time (e) and became detrapped eventually (f).

### 3.3 Selective melting of Au nanorods

In order to gain a deep insight into the trapping and melting of Au nanorods in the optical trap, we have carried out a series of trapping experiments. Once the trapping experiments were completed, the upper glass slide of the sample cell was removed and the morphologies of the formed structures were examined by using the dark-field mode of the microscope and SEM.

Figure 6(a) shows the SEM image of a typical structure formed by trapping and melting of Au nanorods. A magnified image showing the central part of the structure is presented in Fig. 6(b). A large particle with a diameter of about 500 nm is observed at the centre. It is thought to originate from the merger of a number of melted Au nanorods. Around this large particle, we can see Au clusters with much smaller size and even some unmelted Au nanorods. The distribution of these clusters and nanorods forms two ring structures that surround the central particle. On the two rings indicated by arrows, only clusters formed by melted nanorods are observed. Interestingly, one can easily find unmelted Au nanorods with a very low area density in the space between the central particle and the first ring and that between the two rings. This observation in combination with the TPL pattern of the trapped Au nanorods and the steady trapping of Au clusters around the central particle indicate that the distribution of electric field in the sample cell is a multi-ring-shaped pattern [27]. This unique pattern of electric field distribution creates an optical potential well (or optical trap) of the same shape and leads to the selective trapping, accumulation and melting of Au nanorods in the optical trap.

Very recently, a ripple-like electric field distribution was found by Obara *et al.* around an Au nanosphere irradiated by fs laser [29–32]. It was suggested that such a field distribution originates from the interference between the incident light and the light scattered by the Au nanosphere. A further investigation revealed that electric field distributions with various patterns could be achieved by utilizing particles or structures with different shapes [29–32]. This unique feature can be employed to fabricate micro- or nanostructures by fs laser ablation. This mechanism was also used by us to successfully explain the high spatial frequency periodic surface structures formed on metal surface [33].

In our experiments, a large number of Au nanorods were trapped and subsequently melted at the focus when the laser light was turned on, forming a large particle at the centre of the focus. The size of the central particle increased with time and it reached rapidly to the resonant wavelength of Mie scattering for the trapping light. A ripple-like distribution of electric field was created around the central particle, similar to the case discussed in Ref [29].

This kind of field distribution will dominate the following trapping and melting processes of Au nanorods and clusters. Since the shape of the central particle is not round, the distribution and accumulation of Au nanorods and clusters around the central particles (i.e. the shape of the rings) is not round, as can be seen in Fig. 6(a). The shape of the central particle also influences the shapes of the orbits where Au clusters are trapped, as manifested in Figs. 4 and 5. Although the laser light with linear polarization was used in the trapping experiments, we could not identify the alignment of single Au nanorods during the trapping processes. When the trapping and melting experiments were completed, we did not observe the preferential alignment of Au nanorods on the conductive glass because the distribution and alignment of Au nanorods was eventually determined by the interfering optical field.

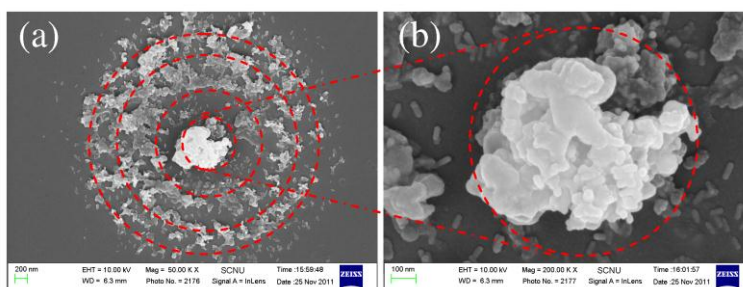


Fig. 6. (a) SEM image of a typical structure formed by trapping and melting of Au nanorods. It shows a large particle at the centre surrounded by two rings. (b) A further magnification of (a) showing the existence of unmelted Au nanorods in between the central particle and the first ring.

#### 4. Summary

We have investigated the trapping and melting of a large number of Au nanorods by using a single focused fs laser light which is in resonance with the LSPR of Au nanorods. The TPL from the trapped Au nanorods was utilized to monitor the trapping and melting processes of Au nanorods. A multi-ring-shaped pattern was observed in the steady state and the central part of the focus generally appeared to be dark. Steady trapping of Au clusters in the orbits circling the focus was observed. In addition to the repulsive interaction that prevents the Au clusters from coalescing, an attractive interaction that makes them move as a whole in the orbit was also found. The SEM observation confirms the existence of a large particle at the centre of the focus and the ring-like distribution of Au clusters around the central particle. All the phenomena can be interpreted by the ripple-like electric field distribution formed in the experimental setup. It is supported by unmelted Au nanorods found in the space between the central particle and that between the two neighboring rings. The results presented in this work are helpful for understanding the trapping and melting of a large number of Au nanorods that may find applications in the fabrication of nanophotonic functional materials and devices.

#### Acknowledgments

The authors acknowledge the financial support from the National Natural Science Foundation of China (Grant Nos. 10974060, 51171066 and 11111120068) and the program for high-level professionals in the universities of Guangdong province, China.